JOURNAL OF MATERIALS SCIENCE: MATERIALS IN MEDICINE 1 (1990) 171–176

Corrosive properties in experimental Ni–Cu–Mn-based alloy systems for dental purposes

K. WAKASA, M. YAMAKI
School of Dentistry, Department of Dental Materials, Hiroshima University, 1-2-3 Kasumi, Minami-Ku, Hiroshima, 734 Japan

Experimental Ni–Cu–Mn-based alloys containing additives were studied to find their corrosive properties in tarnishing tests. The microstructural features revealed interdendritic areas with small corroded regions. In 30Ni–30Cu–40Mn-based alloys which were respectively substituted by aluminium, tin, aluminium and indium (Al–In), Al–Sn and Al–Sn–In the maximum roughness values in the surface roughness curves ranged from 2.0 to 7.2 μm. Each corrosion-resistant alloy system which contained additive elements of Al–In, Al–Si, Ca–Si–C and P–Fe had a smooth surface with a maximum roughness value of 0.8 to 2.0 μm.

1. Introduction

Non-precious base-metal alloys should be able to resist corrosion and tarnishing in the tarnishing test. The resistance is an important parameter when choosing base-metal alloys for dental applications. *In vitro* corrosion and tarnishing of dental base-metal alloys has been evaluated by a potentiostatic technique [1, 2] and the colour-change vector [3–5]. The observations from both *in vivo* and *in vitro* experiments support the fact that copper sulphide was not generally assumed to be the main corrosion product causing tarnishing in noble-metal crown and bridge alloys [6, 7]. In the alloys the copper-rich phase was observed by *in vitro* tests to be significantly more resistant to corrosion and tarnishing than was the silver-rich matrix [8]. The beneficial effect of copper in Ni–Cu–Mn ternary alloys has been demonstrated for tarnishing resistance [4]. The ternary Ni–Cu–Mn alloys had better castability during dental casting [9], and the hardness ranged approximately from 180 to 290 when the nickel contents in the ternary alloys varied from 20 to 50 wt % [10]. The solubilities of nickel and copper were examined when alloy elements were added to the ternary alloys showing that lower solubilities of nickel and copper were obtained [11]. The corrosivity of ternary Ni–Cu–Mn alloys and the improved alloys containing alloying elements has to be clarified from the viewpoint of the microstructural features of the alloys. The aim of this work was therefore to examine the corrosive properties of microstructure in experimental Ni–Cu–Mn-based alloys.

2. Materials and methods

Five experimental alloys were made by vacuum-melting the individual elements: 20 wt % Ni–40 wt % Cu–40 wt % Mn (alloy 1, melting temperature 970° C), 30Ni–30Cu–40Mn (alloy 2, 1000° C), 30Ni–40Cu–30Mn (alloy 3, 1050° C), 40Ni–30Cu–30Mn (alloy 4, 1075° C) and 50Ni–30Cu–20Mn (alloy 5, 1160° C). The alloy compositions and designations were the same as those reported in previous studies [4, 10, 12]. One alloy, which was a 30Ni–30Cu–40Mn-based alloy, was melted with 5 wt % aluminium, 5 wt % aluminium and 5 wt % tin (denoted as 5Al–5Sn), 5 wt % aluminium, 0.1 wt % indium and 4.9 wt % tin (5Al–0.1In–4.9Sn), 5Al–2.5In–2.5Sn, 5Al–4.9In–0.1Sn and 5Al–5In by substituting their alloy elements to manganese content (Table I). The commercial Ni–Cr-based alloy as a control material (Fittloy 50 Type 1, Sankin Ind., Tokyo; control, melting temperature 965° C) was typical for low-fusing casting alloys of this kind on the market in Japan. As additional materials which have previously been reported [11], three of the ternary Ni–Cu–Mn alloys (alloys 1, 4 and 5) were melted by adding alloying elements such as 5Al–5In, denoted as Al–In, Al–Si as a compound additive, Ca–Si–C (compound) and P–Fe (compound) to their alloys by 10 wt %. These alloys are denoted as alloy systems 1, 4 and 5 in this study, as used previously (1, 18Ni–36Cu–36Mn–10 wt % additive; 4, 36Ni–27Cu–27Mn–10 wt % additive; 5, 45Ni–27Cu–18Mn–10 wt % additive) [11].

The materials investigated were examined for both surface roughness after immersion in the solutions and their microstructural characteristics by means of optical and electron microscopy. The tarnishing tests in 0.05% HCl (pH 2.0) and 0.1% sodium sulphide solution (pH 12.0) were done at 37 ± 1° C [13, 15, 16]. After immersing the specimens (15 mm × 20 mm × 2.5 mm), which were cast reported in [4], into the tarnishing solutions (1% lactic acid, pH 2.3; Ringer's solution, pH 6.7 and artificial saliva, pH 11.2) the maximum roughness was evaluated from surface roughness curves (Kosaka Lab., Tokyo, Japan) using the solutions measured in nickel and copper solubilities [11, 13–16]. The colour-change vector was not determined in this study, because the ternary Ni–Cu–Mn alloys had better tarnishing-resistance [4]. Thus, the microstructural changes in the tarnishing tests were examined, especially for the corroded structure.

0957–4530/90 $03.00 + .12

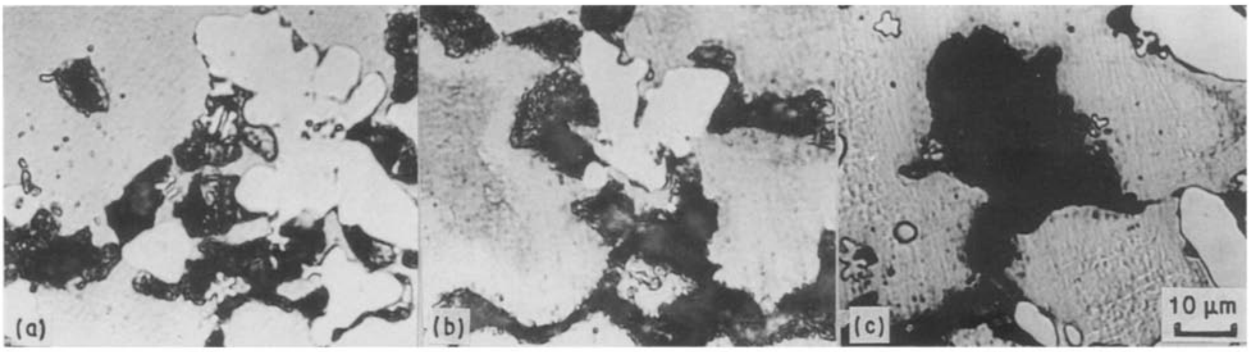

Figure 1 Microstructures of a control material when immersed in 0.05% HCl solution for (a) 1, (b) 2 and (c) 3 days.

3. Results

The microstructural observations of the tarnished alloys in 0.05% HCl solution are shown in Fig. 1 (a control material immersed for 1, 2 and 3 days in the solution) and Fig. 2 (six experimental 30Ni–30Cu–40Mn-based alloys immersed for 3 days in 0.05% HCl). The specific phase was attacked gradually with a dark shade in Fig. 1, whereas the experimental alloys were selectively corroded at interdendritic areas (Fig. 2), Lightly corroded areas were observed for the experimental alloys when immersed in 0.1% sodium sulphide (Fig. 3). The 30Ni–30Cu–40Mn-based alloys containing 5Al–0.1In–4.9Sn, 5Al–2.5In–2.5Sn and 5Al–4.9In–0.1Sn as additive elements were partially corroded at the interdendritic regions when immersed in 0.05% HCl (Fig. 4). Each mapping image in the alloy systems which were immersed for 3 days in 1% lactic acid showed segregation of each additive element at interdendrite area, revealing in secondary electron imaging that the interdendritic area was corroded (Figs 5 to 7). The maximum roughness in ternary Ni–Cu–Mn alloys and a control material ranged approximately from 5 to 17 μm (Table I). The 30Ni–30Cu–40Mn-based alloys showed maximum roughness values ranging from 2.0 to 7.2 μm for those immersed in 0.05% HCl solution (Table II). In Tables III to V the maximum roughness values calculated from surface roughness curves of the tarnished alloy systems are given. The addition of alloying elements to the ternary alloys gave a decrease in the values of the tarnished surface roughness due to the tarnishing test, and the values when immersed in 1% lactic acid were smaller than those in the control material.

4. Discussion

The microstructures in ternary Ni–Cu–Mn alloys were different for 20Ni–40Cu–40Mn and 30Ni–30Cu–40Mn (dendrite structure), and the other alloys (cellular structure) [12]. The ternary 30Ni–30Cu–40Mn alloy was the second strongest material among

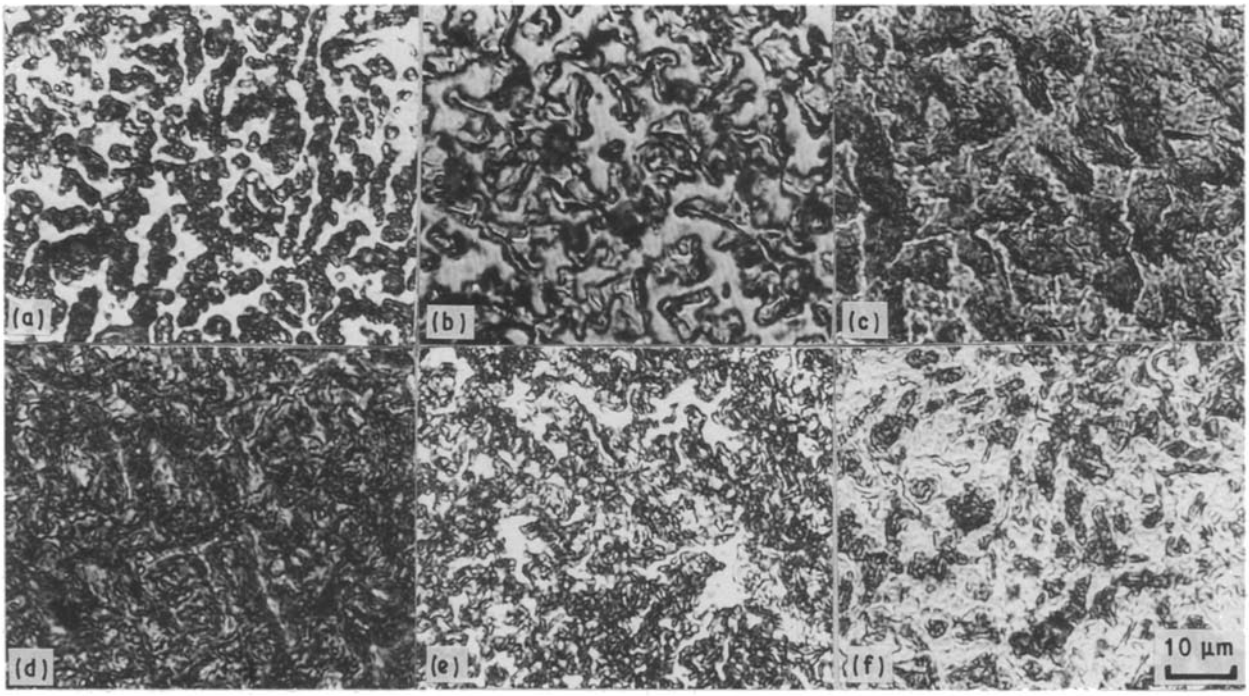

Figure 2 Microstructures of experimental Ni–Cu–Mn-based alloys when immersed for 3 days in 0.05% HCl solution. (a) 30Ni–30Cu–35Mn–5Al, (b) 30Ni–30Cu–30Mn–10Al, (c) 30Ni–30Cu–35Mn–5Sn, (d) 30Ni–30Cu–30Mn–10Sn, (e) 30Ni–30Cu–30Mn–5Al–5In and (f) 30Ni–30Cu–30Mn–5Al–5Sn.

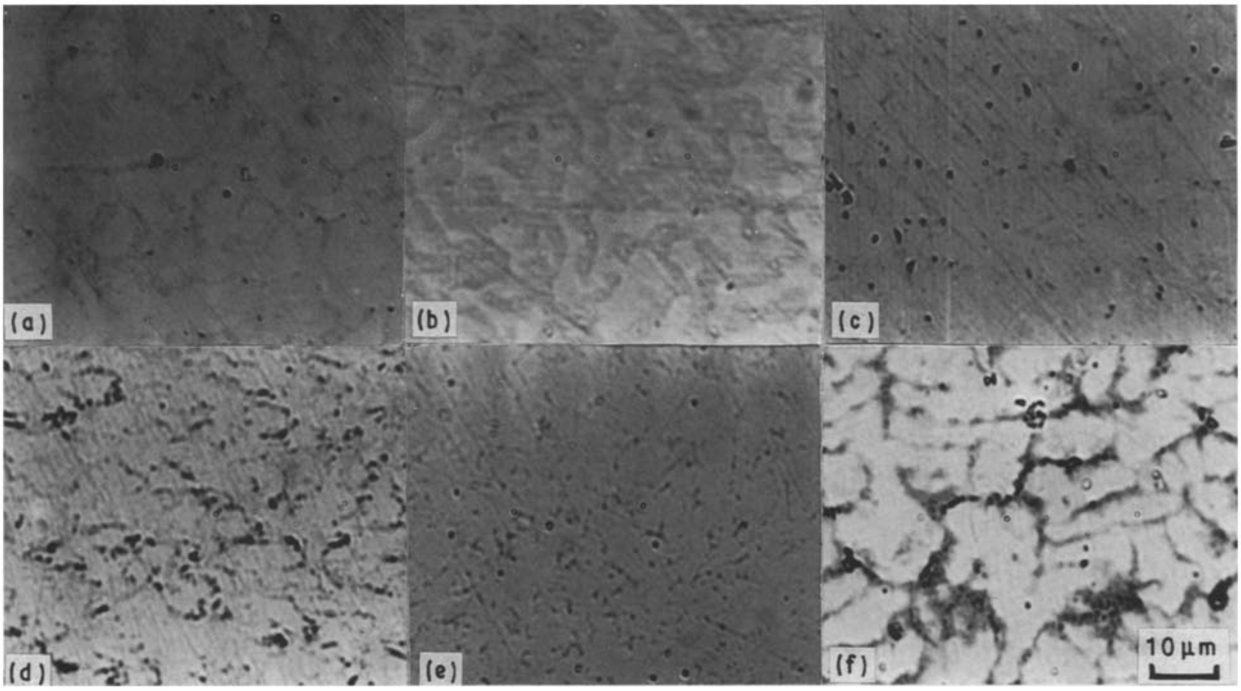

Figure 3 The observed results for the Ni–Cu–Mn-based alloys in 0.1% sodium sulphide (3 days immersion). (for key, see Fig. 2.)

the five ternary alloys in tensile test [10]. The 30Ni–30Cu–40Mn-based alloy containing, respectively, aluminium, tin, Al–In and Al–Sn showed corrosivity at interdendritic areas (Fig. 2). By electron microscopy (Figs 5 to 7) it could be seen that the alloy systems containing additive elements were selectively corroded, and the corroded areas corresponded to the interdendritic region. Visual inspection in a commercial nickel-based alloy, which was immersed in 0.05% HCl solution, showed clearly that the corroded area was attacked locally over the grains (Fig. 1). The tarnishing tests (0.05% HCl and 0.1% sodium sulphide solutions) clarified the finding of locally corroded areas in experimental Ni–Cu–Mn-based alloys (Figs 2 to 4).

These alloys had small surface roughness values (2.0 to 7.2 µm) over the corroded surface (Table II). A decrease in the surface roughness was obtained for alloys containing additive elements compared with the maximum roughness in ternary Ni–Cu–Mn alloys when immersed in 1% lactic acid (Tables I and III). The quantitative appearance of corroded specimens subjected to tarnishing-testing due to 1% lactic acid was different, showing that the maximum roughness value ranged from 0.8 to 2.0 µm in improved Ni–Cu–Mn-based alloys containing alloying additives such as Al–In, Al–Si, Ca–Si–C and P–Fe. These maximum roughness values in the surface roughness curves correlated well with the corrosivity in the interdendritic region. This observation was also found for low-gold Ag–Pd–Cu–Zn alloys which showed corroded interdendritic positions such as both Pd–Cu–Zn-rich compound particles and silver-rich phase [7, 8, 17].

In the low-gold alloys, the corrosion and the tarnishing seem to have taken place predominantly in areas of local galvanic cells between the anode (silver-rich phase) and the cathode (Pd–Cu–Zn-rich particles) [8]. This study showed that the improved Ni–Cu–Mn alloy systems had corroded interdendritic areas and their areas corresponded to the segregated positions

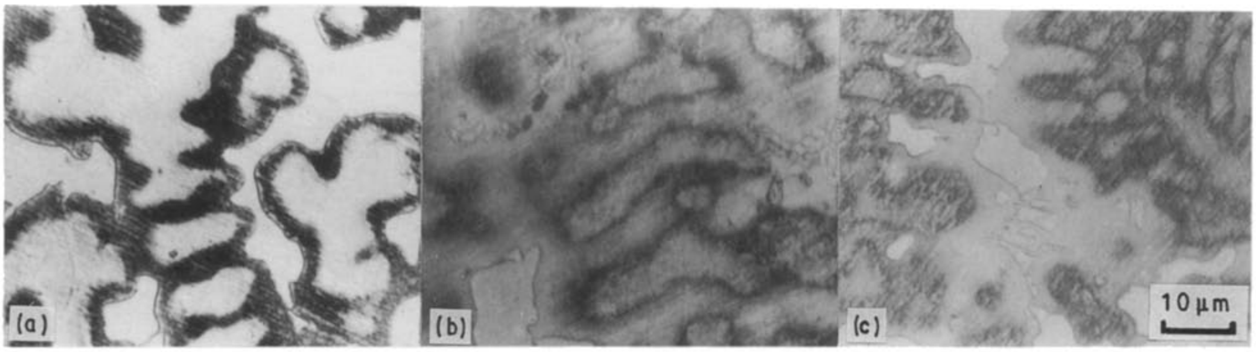

Figure 4 Microstructures in experimental Ni–Cu–Mn-based alloys (3 days, 0.05% HCl): (a) 30Ni–30Cu–30Mn–5Al–0.1In–4.9Sn, (b) 30Ni–30Cu–30Mn–5Al–2.5In–2.5Sn and (c) 30Ni–30Cu–30Mn–5Al–4.9In–0.1Sn.

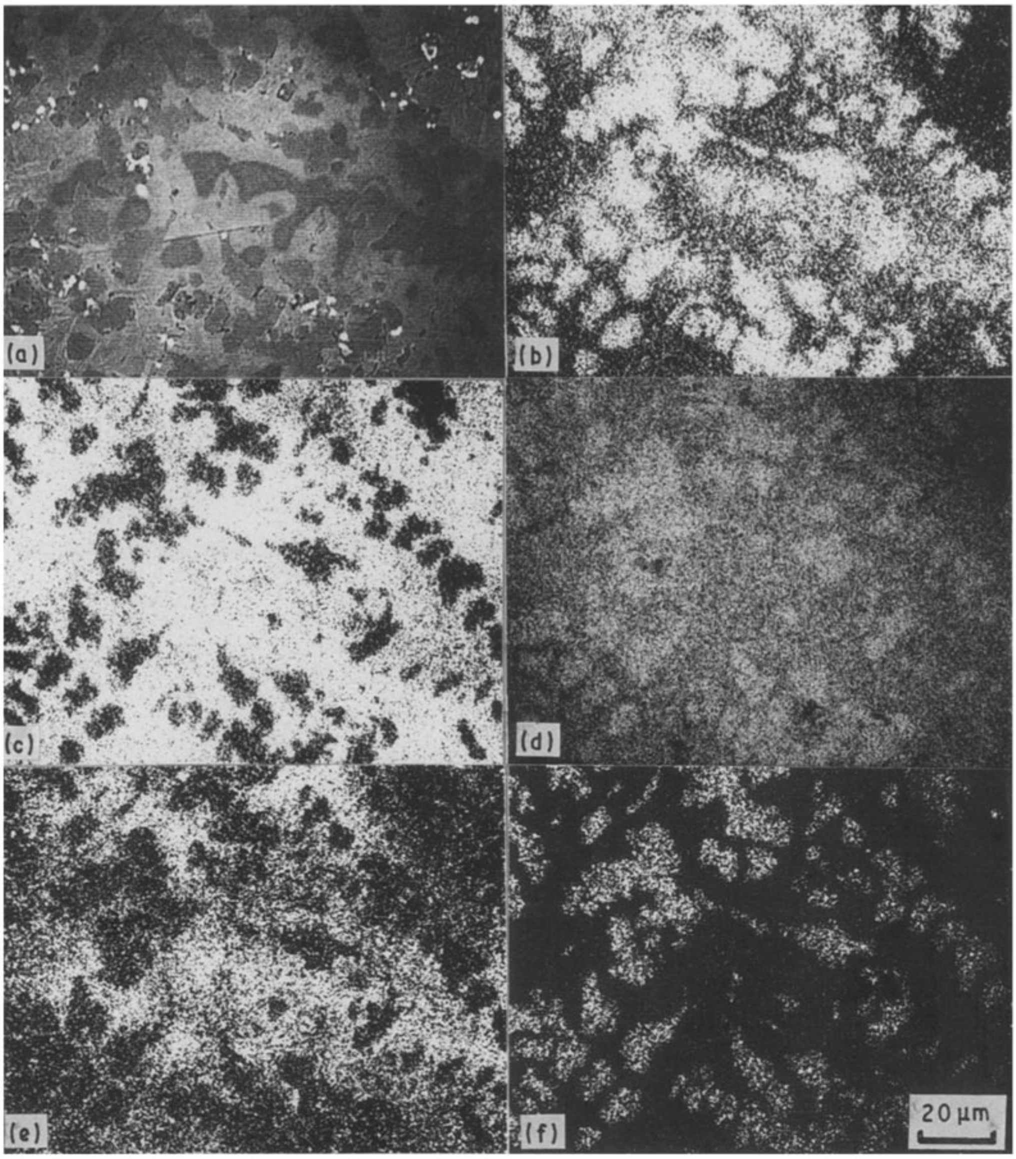

Figure 5 Electron microscopy in alloy system 1 containing additive Al–Si (3 days, 1% lactic acid). (a) Secondary electron image, (b) nickel-, (c) copper-, (d) manganese-, (e) aluminium- and (f) silicon-mapping images.

(Figs 5 to 7). When alloying elements were added to the ternary alloys, additive elements such as silicon, indium and phosphorus segregated in the interdendritic area of the Ni–Cu–Mn-based alloys. As microgalvanic cells could be formed over short distances, the existence of the interdendritic region would be important in this study. It was not deduced which was the cathodic or anodic site, but the finding of a corroded interdendritic area would support the formation of the sites. For the Ni–Cu–Mn-based alloy systems, the best overall resistance to corrosion in the tarnishing-testing was observed for the solutionized conditions investigated. These alloy systems had alloying additives such as Al–In, Al–Si, Ca–Si–C and

TABLE I Maximum roughness calculated from surface roughness curves in ternary Ni–Cu–Mn alloys and a control material, which were immersed for 3 days in 1% lactic acid

Material	Maximum roughness (μm)
20Ni–40Cu–40Mn	2.4 ± 0.2
30Ni–30Cu–40Mn	10.8 ± 0.4
30Ni–40Cu–30Mn	11.4 ± 0.3
40Ni–30Cu–30Mn	16.2 ± 0.5
50Ni–30Cu–20Mn	16.8 ± 0.4
Control	5.0 ± 1.0

TABLE II The values of maximum roughness in each Ni–Cu–Mn-based alloy containing aluminium, tin, Al–In, Al–Sn and Al–In–Sn, which were immersed for 3 days in 0.05% HCl solution

Material	Maximum roughness (μm)
30Ni–30Cu–35Mn–5Al	4.2 ± 0.1
30Ni–30Cu–30Mn–10Al	6.5 ± 0.5
30Ni–30Cu–35Mn–5Sn	7.0 ± 0.3
30Ni–30Cu–30Mn–10Sn	7.2 ± 0.2
30Ni–30Cu–30Mn–5Al–5In	2.0 ± 0.2
30Ni–30Cu–30Mn–5Al–5Sn	3.4 ± 0.4
30Ni–30Cu–30Mn–5Al–0.1In–4.9Sn	5.2 ± 0.7
30Ni–30Cu–30Mn–5Al–2.5In–2.5Sn	6.8 ± 0.6
30Ni–30Cu–30Mn–5Al–4.9In–0.1Sn	6.7 ± 0.4

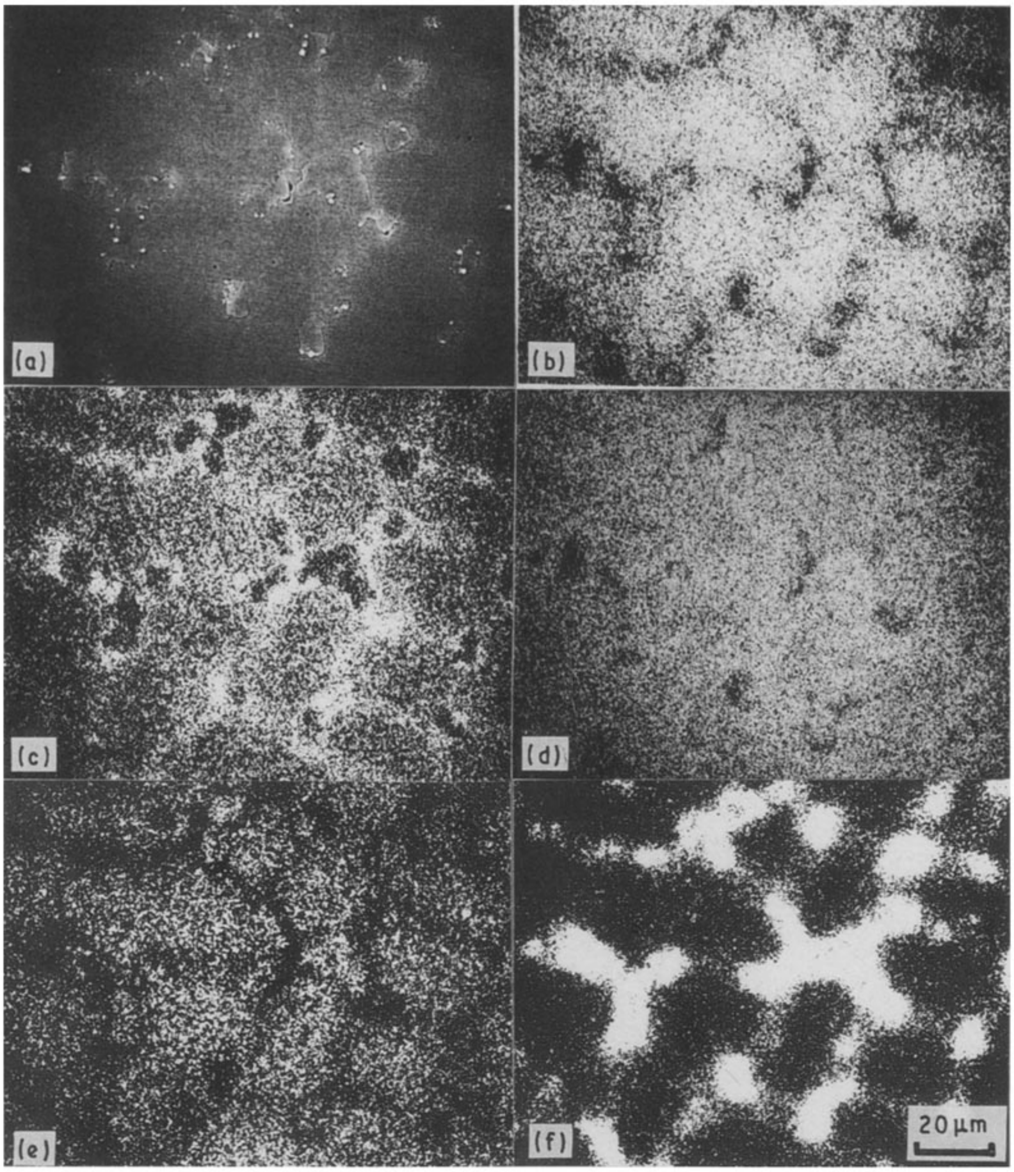

Figure 6 Electron microscopy in alloy system 4 containing additive Al–In (3 days, 1% lactic acid). (a) Secondary electron image, (b) nickel-, (c) copper-, (d) manganese-, (e) aluminium- and (f) indium-mapping images.

P–Fe. Compared with the ternary Ni–Cu–Mn alloys, the values of maximum roughness were very low, and the greatest corrosion resistances were expected for the improved Ni–Cu–Mn-based alloy systems; in their microstructures, the interdendritic areas were important to their corrosive properties.

These results support their application to the dental field, indicating better corrosive resistance than the conventional nickel-based alloy and ternary Ni–Cu–

TABLE III Maximum roughness (μm) in experimental Ni–Cu–Mn-based alloy systems immersed for 3 days in 1% lactic acid (for key, see text)

Alloy system	Additive element			
	Al–In	Al–Si	Ca–Si–C	P–Fe
1	1.5 ± 0.2	0.8 ± 0.1	1.3 ± 0.3	0.9 ± 0.1
4	1.2 ± 0.2	0.9 ± 0.2	1.2 ± 0.3	0.9 ± 0.2
5	0.8 ± 0.1	0.8 ± 0.1	2.0 ± 0.2	1.5 ± 0.2

TABLE IV Maximum roughness values (μm) (3 days, Ringer's solution)

Alloy system	Additive element			
	Al–In	Al–Si	Ca–Si–C	P–Fe
1	1.3 ± 0.1	0.6 ± 0.3	1.1 ± 0.2	0.8 ± 0.1
4	1.1 ± 0.1	0.8 ± 0.2	1.0 ± 0.3	0.7 ± 0.1
5	0.7 ± 0.2	0.7 ± 0.1	1.8 ± 0.2	1.2 ± 0.2

TABLE V Maximum roughness values (μm) (3 days, artificial saliva)

Alloy system	Additive element			
	Al–In	Al–Si	Ca–Si–C	P–Fe
1	1.1 ± 0.1	0.7 ± 0.1	1.6 ± 0.2	1.5 ± 0.2
4	1.1 ± 0.1	2.0 ± 0.1	1.4 ± 0.1	1.3 ± 0.2
5	1.2 ± 0.1	0.8 ± 0.2	0.7 ± 0.1	1.0 ± 0.2

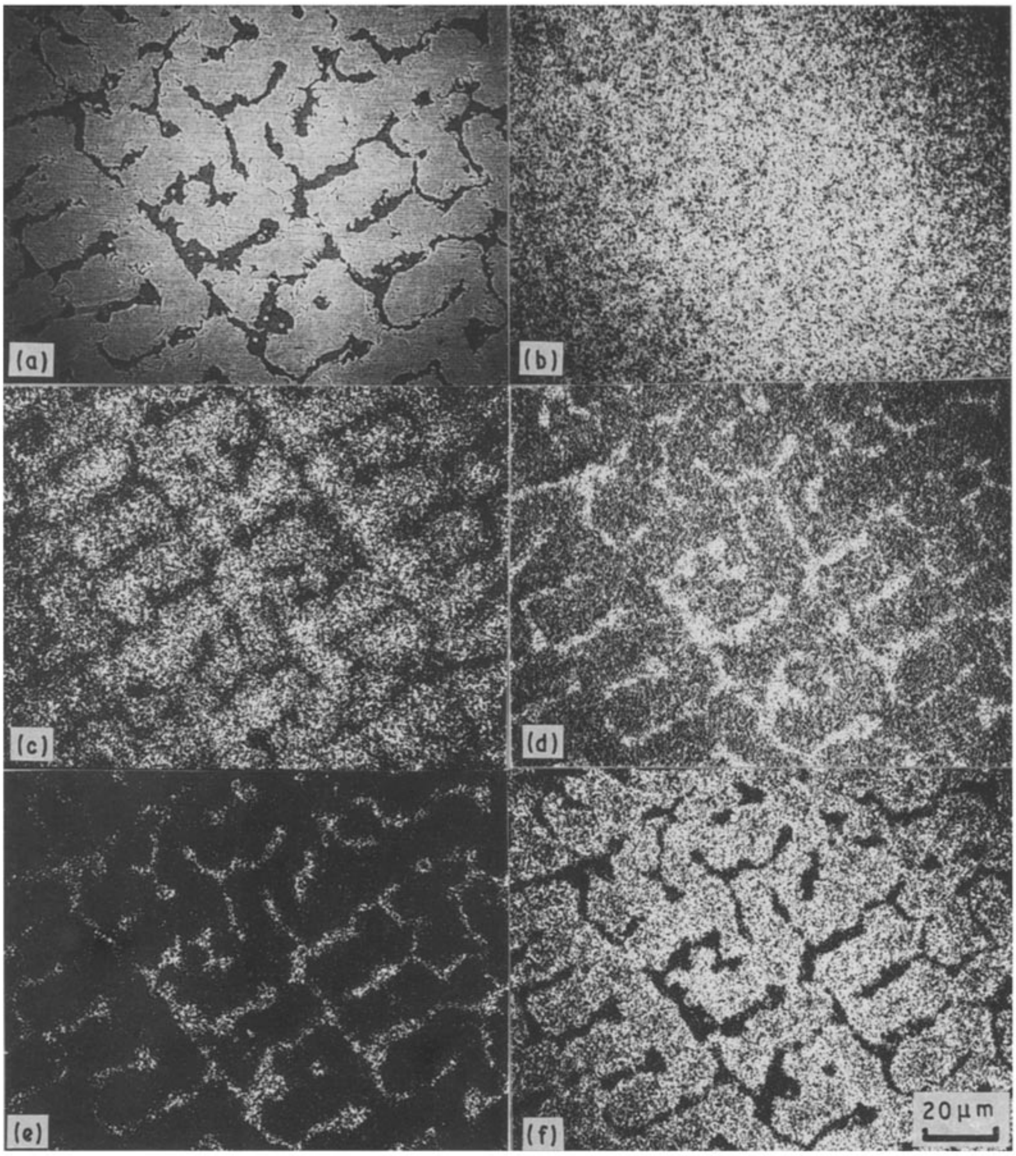

Figure 7 Electron microscopy in alloy system 5 containing P–Fe additive (3 days, 1% lactic acid). (a) Secondary electron image, (b) nickel-, (c) copper-, (d) manganese-, (e) phosphorus- and (f) iron-mapping images.

Mn alloys. The experimental ternary Ni–Cu–Mn alloys could be changed to dental alloy systems by minor alloying additions.

References

1. P. J. ARAGON and S. F. HULBERT, *J. Biomed. Mater. Res.* **6** (1972) 155.
2. J.-M. MEYER and J.-N. NALLY, *J. Dent. Res.* **54** (1975) Special Issue No. L452.
3. T. HORIBE, *et al.*, *Shika Zairyou Kikai* **3** (1984) 605.
4. B. I. SOSROSOEDIRDJO, K. WAKASA and M. YAMAKI, *J. Mater. Sci.* **24** (1989) 1243.
5. S. ESPEVIK, *Acta Odontol. Scand.* **36** (1978) 113.
6. R. W. PHILLIPS, "Skinner's Science of Dental Materials", 8th Edn (W. B. Saunders & Co., Philadelphia) p. 299.
7. H. HERØ and L.NIEMI, *J. Dent. Res.* **65** (1986) 1303.
8. L. NIEMI and H. HERØ, *ibid.* **64** (1985) 1163.
9. K. WAKASA and M. YAMAKI, *J. Mater. Sci. Mater. Med.* **1** (1990) 90.
10. B. I. SOSROSOEDIRDJO, K. WAKASA and M. YAMAKI, *J. Mater. Sci.* **24** (1989) 3667.
11. K. WAKASA, B. I. SOSROSOEDIRDJO and M. YAMAKI, *ibid.* **25** (1990) 2159.
12. B. I. SOSROSOEDIRDJO, K. WAKASA and M. YAMAKI, *ibid.* **24** (1989) 1247.
13. V. J. COLANGELO and N. D. GREENE, *J. Biomed. Mater. Res.* **3** (1969) 247.
14. H. J. MUELLER and F. H. GREENER, *ibid.* **4** (1970) 29.
15. J. HASEGAWA, *Shika Zairyou Kikai* **3** (1984) 547.
16. M. MATSUMURA, *Hotetsu-shi* **30** (1986) 1198.
17. H. HERØ and J. VALDERHAUG, *J. Dent. Res.* **64** (1985) 139.
18. A. J. LEVIS, *Aust. Dent. J.* **23** (1978) 275.
19. G. BARAN and E. C. WOODLAND, *J. Dent. Res.* **60** (1981) 1761.

Received 12 January
and accepted 1 February 1990